Article

Effects of a Ring-Size and Polar Functional Groups on the Glutathione Peroxidase-Like Antioxidant Activity of Water-Soluble Cyclic Selenides

Kenta Arai, Fumio Kumakura, Motoi Takahira, Natsumi Sekiyama, Nozomi Kuroda, Toshiki Suzuki, and Michio Iwaoka

Just Accepted

Effects of a Ring-Size and Polar Functional Groups on the Glutathione Peroxidase-Like Antioxidant Activity of Water-Soluble Cyclic Selenides
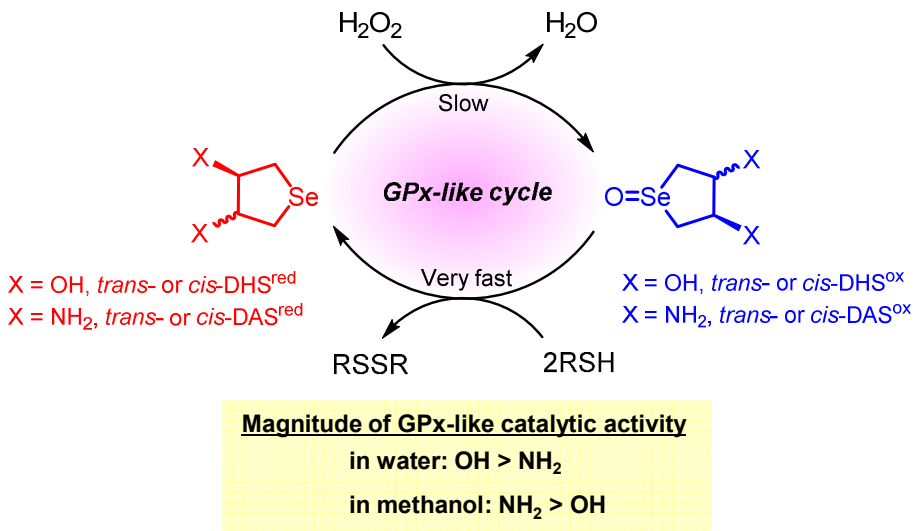
Kenta Arai, Fumio Kumakura, Motoi Takahira, Natsumi Sekiyama, Nozomi Kuroda, Toshiki Suzuki, and Michio Iwaoka*

Department of Chemistry, School of Science, Tokai University, Kitakaname, Hiratsuka-shi, Kanagawa 259-1292, Japan.

Corresponding Author

*E-mail: miwaoka@tokai.ac.jp (M. I.).

TOC/Abstract graphic

ABSTRACT: To elucidate the effects of ring structure and a substituent on the glutathione peroxidase (GPx)-like antioxidant activity of aliphatic selenides, series of water-soluble cyclic selenides with a variable ring-size and polar functional groups were synthesized, and their antioxidant activities were evaluated by the NADPH-coupled assay using H_2O_2 and glutathione (GSH) in water and also by the NMR assay using H_2O_2 and dithiothreitol (DTT^{red}) in methanol. Strong correlations were found among the GPx-like activity in water, the second-order rate constants for the oxidation of the selenides, and the HOMO energy levels calculated in water. The result supported that the oxidation process is a rate-determining step of the catalytic cycle. On the other hand, such correlations were not obtained for the activity observed in methanol. The optimal ring-size was determined to be five. A sort of a substituent ($NH_2 < OH < CO_2H$) and the count can also control the activity, whereas the stereo configuration has only marginal effects on the activity in water. In methanol, however, the activity rank could not be explained by the simple scenarios applicable in water.

Introduction

Selenium (Se), a member of group 16 chalcogen elements, is an essential micronutrient for living organisms. Generally, selenium is involved in proteins as selenocysteine (Sec), which is a selenium analog of natural amino acid cysteine (Cys) and is genetically coded like other

2

proteinogenic amino acids.[1] Significant roles of selenium-containing proteins are implicated in

maintenance of redox homeostasis in cells. Glutathione peroxidase (GPx), a representative

selenoenzyme, catalyzes reduction of reactive oxygen species (ROS), such as hydrogen peroxide

(H_2O_2), to harmless water (H_2O) using glutathione (GSH) as a reducing cofactor.[2–5] In the past

few decades, synthesis and application of low molecular weight organoselenium compounds as

possible GPx mimics have been explored in fields of chemical biology.[6–11] For example,

aromatic diselenides (ArSeSeAr) having a polar substituent, such as OH and NH_2, near the

selenium atom can imitate the catalytic cycle of GPx and exhibit significant GPx-like antioxidant

activity.[12–19] For such GPx mimics, selection of a polar substituent is one of important factors to

control the activity because it can regulate the reactivity and stability of the intermediates, which

appear during the catalytic cycle, through weak nonbonded $Se \cdots X$ (X = O, N, etc.) interaction

and/or inductive electronic perturbation.

On the other hand, monoselenides (RSeR) have less frequently been focused as potential GPx

mimics. However, selenides can be oxidized with H_2O_2 to the corresponding selenoxides, and the

selenoxides can be reduced back to the selenides with thiols (RSH). This selenide–selenoxide

redox system indeed provides a unique catalytic cycle (Scheme 1) analogous to GPx.[20,21]

Rahmanto and Davies investigated the GPx-like activity of selenomethionine to reduce protein

hydroperoxides.[22] Back reported high GPx-like activity of bis(3-hydroxypropyl) selenide, which

forms a reactive spiro dioxoselenurane species, instead of a selenoxide, when oxidized.[23] Braga

3

recently characterized in the oxidation products of aryl benzyl selenides in methanol a highly

reactive hydroxy perhydroxy selenane species (RR'Se(OH)OOH), which would be a key

intermediate for the observed significant GPx-like catalytic activity.[24]
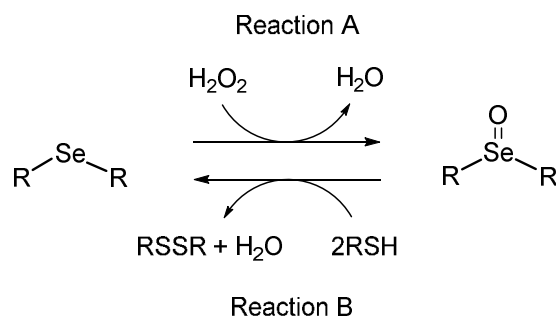
Scheme 1: A GPx-like redox cycle of selenides.

We recently found that the GPx-like antioxidant activity of water-soluble aliphatic selenides

having various polar functional groups (X) (Scheme 2) critically depends on X: the activity

increases in the order of **2** (NH_2) < **1** (OH) < **3** (CO_2H) in an aqueous medium, while the order is

inverted in methanol, i.e., **3** (CO_2H) < **1** (OH) < **2** (NH_2).[21] Similar substituent effects were

reported on the GPx-like activity of other series of simple aliphatic selenides.[25] It was also

indicated that the rate-determining step of the catalytic cycle is the oxidation of the selenide (i.e.,

Reaction A in Scheme 1) and the reduction of the selenoxide (i.e., Reaction B in Scheme 1)

proceeds rapidly.[21,26] Furthermore, cyclic selenide **4** (*trans*-DHS[red])[27] exhibited higher GPx-like

4

activity in both water and methanol than open-chain selenide **1**. The activity enhancement

observed for **4** was attributed to the cyclic structure, which would modify the HOMO so that the

oxidation of **4** takes place more effectively.[21] In this context, the cyclic selenides having a polar

functional group other than OH would be interesting synthetic targets to enhance the GPx-like

activity.

1: X = OH
2: X = NH$_2$
3: X = CO$_2$H

trans-DHS^{red} (**4**)
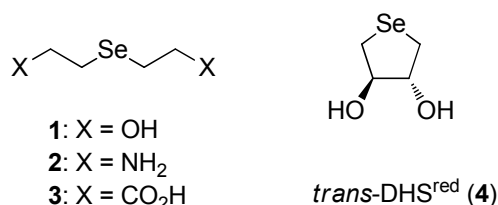
Scheme 2: Water-soluble selenides previously studied.

In the present study, to elucidate more clearly the effects of ring structure and polar functional

groups on the GPx-like antioxidant activity of selenides, series of water-soluble cyclic selenides

5-11 (Scheme 3) with a variable ring-size and substituents have been synthesized, and their redox

behaviors are compared with those of **1-4** as reference compounds. The effects of stereo

configuration (i.e., **4** vs. **6** and **9** vs. **10**) and a count of a substituent (i.e., **8** vs. **9** or **10**), as well as

the solvent effects, are discussed based on reducing ability of the selenides (i.e., the ability as

reducing agents) and the HOMO energy levels.

5
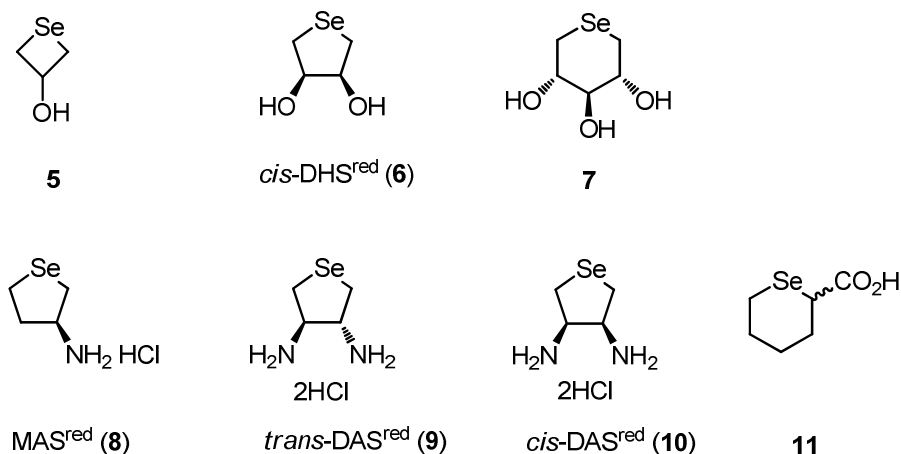
Scheme 3: Water-soluble cyclic selenides examined in this study.

Results and Discussion

Synthesis of water-soluble cyclic selenides. Hydroxy-substituted four-membered cyclic selenide **5**,[28] hydroxyl-substituted six-membered cyclic selenide **7**,[29,30] and carboxy-substituted six-membered cyclic selenide **11**[20] were synthesized according to the literature procedures. Five-membered cyclic selenide **8** (monoaminoselenolane, MAS[red]) was obtained as a hydrochloride salt from L-aspartic acid in six steps.[31] On the other hand, cyclic selenide **6** (*cis*-dihydroxyselenolane, *cis*-DHS[red]), which corresponds to a *cis* stereoisomer of *trans*-DHS[red] (**4**), was synthesized according to Scheme 4. Dibenzyl ether **12** was prepared from *cis*-2-butene-1,4-diol in two steps by following the literature procedures.[32] After conversion of **12** to an acetonide form (**13**),[33] the benzylic groups (Bn) were removed reductively. Produced

diol **14** was then treated with methanesulfonyl chloride (MsCl) to give dimesylate **15**.[34]

cis-DHS[red] (**6**) was obtained by selenation of **15** with sodium hydrogen selenide (NaHSe) and

subsequent deprotection of the acetonide group. The total yield of **6** was 37% from **12**.

cis-DHS[red] (**6**) is a known compound, but the synthetic route in this study is different from the

previous one[35].
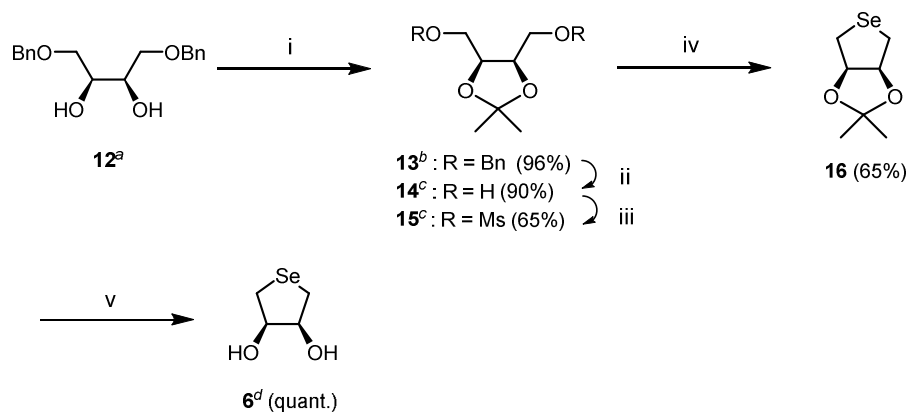
Scheme 4: Synthesis of *cis*-DHS[red] (**6**). Reagents and conditions: i) DMP, *p*-TsOH, acetone, rt,

1.5 h; ii) H$_2$, Pd/C, MeOH, rt, 23 h; iii) MsCl, pyridine, 0 °C, 2.5 h; iv) NaHSe, EtOH/THF,

reflux, 4 h; v) AcOH, MeOH, reflux, 19 h. [a]Ref 32, [b]Ref 33, [c]Ref 34, [d]Ref 35

Diaminoselenolanes, i.e., *trans*-DAS[red] (**9**) and *cis*-DAS[red] (**10**), with five-membered ring

structure were synthesized as dihydrochloride salts according to Scheme 5. Starting from diols

17a and **17b**, which were prepared in eight and seven steps, respectively, from

cis-2-butene-1,4-diol by following the literature procedures,[36–39] target selenides **9** and **10** were

obtained in three steps through mesylation and selenation of the hydroxyl groups and subsequent

7

deprotection of the Boc groups. The total yields of **9** and **10** were 73 and 85%, respectively, from

17. Synthesis of *cis*-DAS[red] (**10**) was previously reported,[36] but our synthetic route was slightly

modified from previous one. All cyclic selenides (**5-11**) obtained in this study were

unambiguously characterized by ^{1}H, ^{13}C, and ^{77}Se NMR spectroscopy and HRMS (APCI+)

analyses (see the experimental section for details).
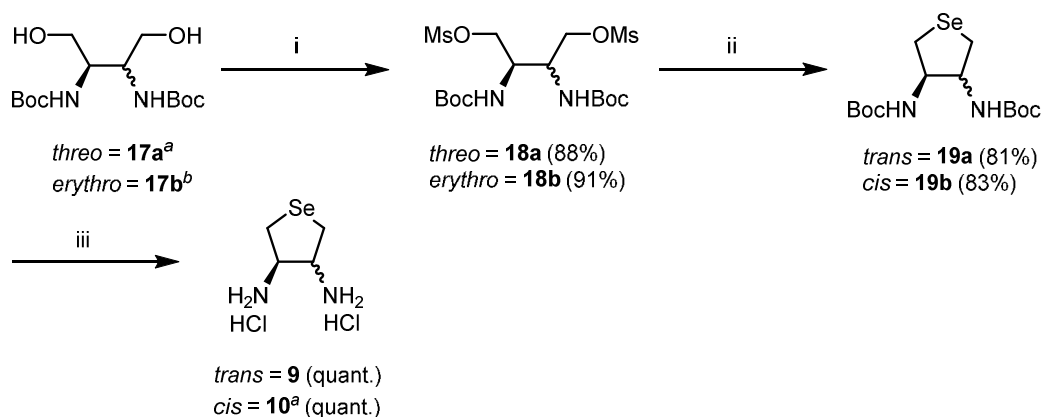
Scheme 5: Synthesis of *cis*- and *trans*-DAS[red]. Reagents and conditions: i) MsCl, pyridine, 0 °C,

3.5 h; ii) NaHSe, EtOH/THF, reflux, 4 h; iii) HCl, H$_2$O/THF, 30 °C, 18 h. [a]Ref 36. [b]Ref 39
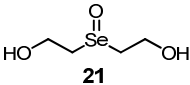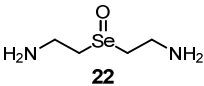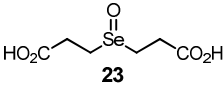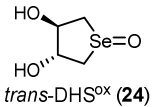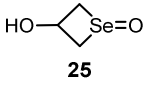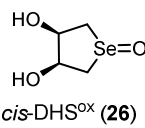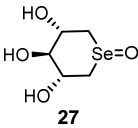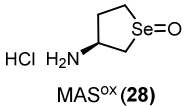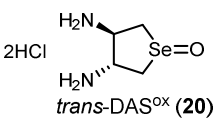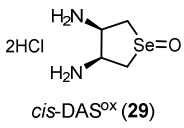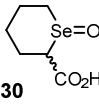
Redox properties of selenides/selenoxides. In order to confirm the redox properties of the

synthesized cyclic selenides (**5-11**), the oxidation and the subsequent reduction (Scheme 1) were

monitored by ^{77}Se NMR spectroscopy in D$_2$O. The spectral changes observed for **9** are shown in

Figure 1. When **9** was reacted with one equivalent of H$_2$O$_2$ for 120 min, the absorption for **9** (δ =

122 ppm) completely disappeared, and a new signal that corresponds to selenoxide *trans*-DAS[ox]

(**20**) appeared at δ = 935 ppm. Subsequently, one equivalent of dithiothreitol (DTT[red]) was added

to the resulting solution as a dithiol substrate to observe quantitative recovery of **9**. In ^{1}H NMR

spectrum, concomitant formation of disulfide DTT (DTT[ox]) was observed (see ^{1}H NMR spectra

in supporting information). These experiments clearly showed that selenide **9** has capacity of a

redox catalyst as a GPx mimic. The other selenides also showed similar redox behaviors. The

^{77}Se NMR chemical shifts observed for the selenides and the corresponding selenoxides are

summarized in Table 1. Although all selenides could be transformed quantitatively to selenoxides,

stability of the selenoxides varied significantly: *cis*-DHS[ox] (**26**), **27**, *trans*-DAS[ox] (**20**), and

cis-DAS[ox] (**29**) were stable as a solid material like *trans*-DHS[ox] (**24**), while MAS[ox] (**28**)

gradually decomposed when precipitated from the solution and selenoxides **25** and **30** degraded

slowly even in solution upon prolonged preservation. It should be noted that some selenoxides

show two absorption signals due to pyramidalization of the selenoxide moiety.

1
2
3
4
5
6
7
8
9
10
11
12
13
14
15
16
17
18
19
20
21
22
23
24
25
26
27
28
29
30
31
32
33
34
35
36
37
38
39
40
41
42
43
44
45
46
47
48
49
50
51
52
53
54
55
56
57
58
59
60
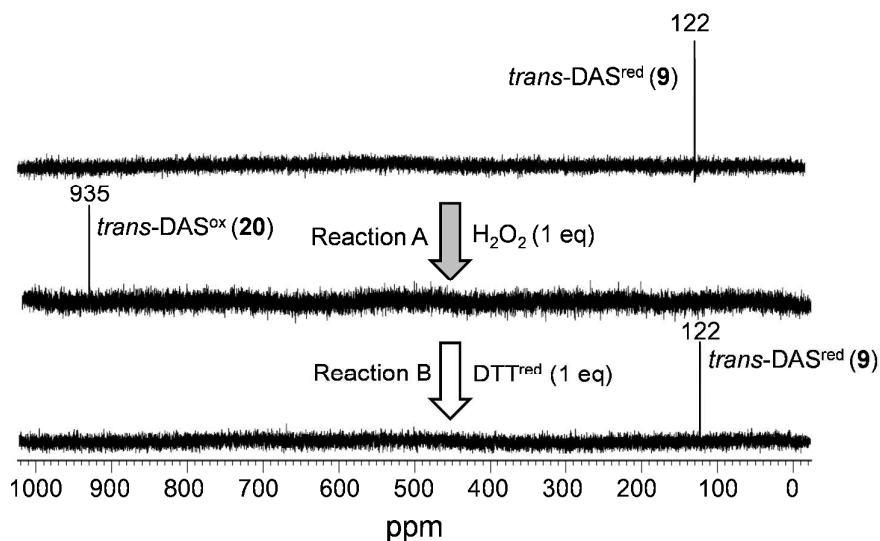
Figure 1: ^{77}Se NMR spectral changes upon oxidation (Reaction A) and subsequent reduction

(Reaction B) of *trans*-DAS^{red} (**9**) in D$_2$O at 25 °C. Reaction conditions were $[\mathbf{9}]_0 = [H_2O_2]_0 = 48$

mM for reaction A, and one equivalent of DTT^{red} was added in reaction B.

Table 1: ^{77}Se NMR chemical shifts of selenides and the corresponding selenoxides

Selenides	δ_{Se} [a]	Selenoxides	δ_{Se} [a]
1	80	**21**	838
2	78	**22**	872
3	179	**23**	865
4	74	*trans*-DHS[ox] (**24**)	926
5	26	**25**	799 (major) and 850
6	84	*cis*-DHS[ox] (**26**)	923 (major) and 925
7	80	**27**	829
8	135	MAS[ox] (**28**)	945 and 958 (major)
9	122	*trans*-DAS[ox] (**20**)	935
10	128	*cis*-DAS[ox] (**29**)	930 and 970 (~1:1)
11	250	**30**	753

11

^{a} ^{77}Se NMR chemical shifts in D_2O.

GPx-like antioxidant activity in an aqueous medium. GPx-like catalytic activity of

selenides **5-11** in a phosphate buffer solution at pH 7.4 was evaluated at 25 °C by the standard

nicotinamide adenine dinucleotide phosphate (NADPH)-coupled method in the presence of

glutathione reductase (GR).[40] In this assay, H_2O_2 is reduced with GSH in the presence of a

catalytic amount of a selenide, and produced disulfide GSSG is reduced with NADPH by the

function of GR enzyme. The velocity of H_2O_2 reduction can be monitored by the decreased

amount of NADPH, which has UV absorption at 340 nm. Figure 2 shows the decrease of the

absorbance at 340 nm as a function of the reaction time. The initial velocities (v_0) estimated from

Figure 2 are summarized in the second column of Table 2.

The activities of open-chain selenide **1** and cyclic selenides **4–7** are compared in Figure 2A to

investigate the ring-size effects on the GPx-like activity. All selenides exhibited the GPx-like

activity under the applied conditions, where excess H_2O_2 with respect to NADPH was added. It

is notable that the activity of cyclic selenides **4–7** was higher than that of selenide **1**,

reconfirming our previous observation that cyclic selenides are more efficient GPx mimics than

open-chain selenides.[21] In addition, the order of the activity, **4** ≈ **6** > **5** > **7** suggested that an

optimal ring-size for the GPx-like activity of cyclic selenides is five. The relative configuration

of the polar substituents (i.e., OH) did not affect the activity because *trans*-DHS[red] (**4**) and

cis-DHS[red] (**6**) showed almost the same activity.

Figure 2B compares the GPx-like activities of **2–4** to **8–11**. As observed above in the case of a

13

OH substituent, the GPx-like activities of cyclic selenides **8**–**10** were higher than that of open-chain selenides **2** when the substituent was NH_2. However, in the case of CO_2H, the activity of six-membered cyclic selenide **11** was similar to or slightly lower than that of open-chain **3**, probably due to the less number of CO_2H present in **11**, in addition to the non-optimal ring-size.

In the meantime, as to the effects of the functional group, the activity of cyclic selenides increased in the order, **9** and **10** (NH_2 ×2) < **4** (OH ×2) < **8** (NH_2 ×1) < **11** (CO_2H ×1). This order is almost consistent with the order observed for open-chain selenides in an aqueous medium, i.e., **2** (NH_2) < **1** (OH) < **3** (CO_2H).[21] Generally, it can be assumed that a negatively charged carboxylic group ($-CO_2^-$) at pH 7.4 would enhance reducing ability of the selenide moiety through inductive electron-releasing, while a positively charged amino group ($-NH_3^+$) would diminish the reducing ability through inductive electron-withdrawing. Therefore, the trend observed for the cyclic selenides can be explained by this simple consideration, except for the case of MAS^{red} (**8**). The reason for the unusual redox behavior of **8** is not clear at this moment.

14
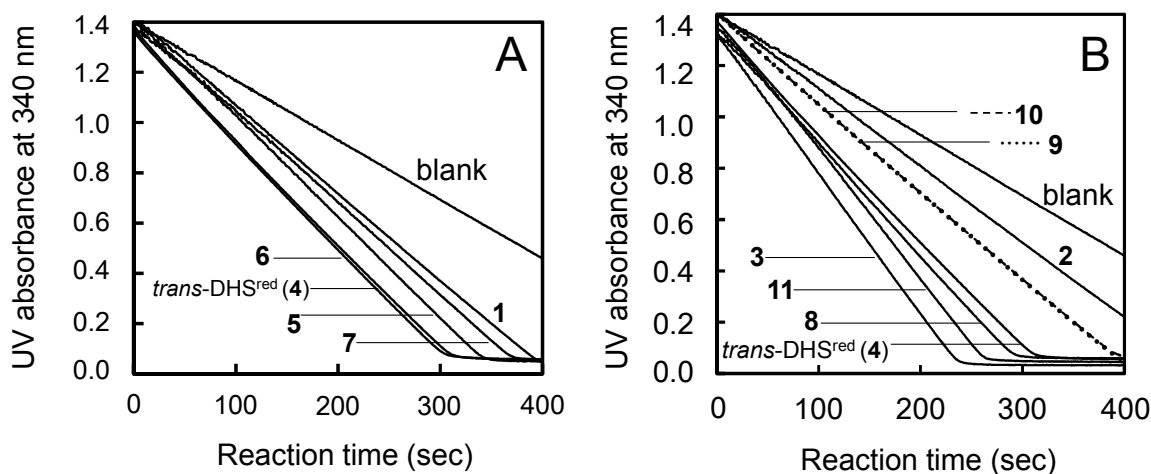
Figure 2: NADPH-coupled GPx assay for water-soluble selenides **1** and **4-7** (A) and **2-4** and

8-10 (B). Reaction conditions were $[GSH]_0 = 1.0$ mM, $[H_2O_2]_0 = 2.5$ mM, $[NADPH]_0 = 0.3$ mM,

$[GR] = 4$ units/mL, and $[selenide] = 0.2$ mM in pH 7.4 phosphate buffer at 25 °C. The results for

selenide **1-4** were quoted from Ref 21.

Table 2: Summary of GPx-like catalytic activity of selenides in water and in MeOH along with the

second-order rate constants for the oxidation and the HOMO energy levels.

Selenides	v_0 (µM min^{-1})^a	t_{50} (min)^b	k_{ox} (M^{-1} s^{-1})^c	HOMO in vacuo (eV)^d	Substituents	HOMO in water (eV)^e	Substituents
No catalyst	32.2 (± 3.2)	>300	-	-			
1	44.2 (± 2.4)	90	0.26 (± 0.02)	−6.07	OH	−6.20	OH
2	34.5 (± 1.1)	10	0.06 (± 0.01)	−5.83	NH_2	−6.69	NH_3^+
3	71.1 (± 6.9)	100	0.87 (± 0.02)	−6.10	CO_2H	−5.72	CO_2^-
trans-DHS^{red} (**4**)	54.2 (± 4.0)	40	0.57 (± 0.03)^f	−6.12	OH_{ax}, OH_{ax}	−6.16	OH_{ax}, OH_{ax}
5	50.7 (± 2.5)	95	ND^g	−5.90	OH_{eq}	−6.06	OH_{eq}
cis-DHS^{red} (**6**)	54.3 (± 3.7)	15	ND^g	−5.86	OH_{eq}, OH_{ax}	−6.01	OH_{eq}, OH_{ax}
7	45.7 (± 1.5)	275	ND^g	−6.20	OH_{eq}, OH_{eq}, OH_{eq}	−6.21	OH_{eq}, OH_{eq}, OH_{eq}
MAS^{red} (**8**)	59.8 (± 1.1)	20	0.47 (± 0.05)	−5.50	NH_{2ax}	−6.44	$NH_{3\ ax}^+$
trans-DAS^{red} (**9**)	47.2 (± 4.3)	6	0.14 (±0.02)	−5.32	NH_{2ax}, NH_{2ax}	−6.87	$NH_{3\ ax}^+$, $NH_{3\ ax}^+$
cis-DAS^{red} (**10**)	48.2 (± 5.3)	65	0.13 (±0.02)	−5.52	NH_{2eq}, NH_{2ax}	−6.88	$NH_{3\ eq}^+$, $NH_{3\ ax}^+$
11	63.8 (± 1.0)	120	ND^g	−6.02	CO_2H_{eq}	−5.74	$CO_2^-{}_{eq}$

16

^{a} Initial velocities (v_0) of H_2O_2 reduction in phosphate buffer at pH 7.4 and 25 ºC. The values

were calculated from the slope of the UV absorbance changes in the range of 0 to 60 sec in

Figures 2A and 2B.

^{b} Reaction times for 50% conversion of DTT^{red} to DTT^{ox} in MeOH. See Figure 3 for the

reaction conditions.

^{c} Second-order rate constants for the oxidation of selenides with H_2O_2 in water at 25 ºC (i.e.

reaction A in Scheme 1).

^{d} HOMO energy levels calculated at B3LYP/6-31+G(d,p) in vacuo.

^{e} HOMO energy levels calculated at B3LYP/6-31+G(d,p) in water using the polarizable

continuum model (PCM).

^{f} Data was quoted from Ref 21.

^{g} Not determined.

GPx-like antioxidant activity in methanol. The activity was evaluated by applying the

NMR method as previously described.[20] The redox reaction between H_2O_2 and DTT^{red} was

initiated by addition of H_2O_2 to a solution of DTT^{red} in CD_3OD containing a catalytic amount of

a selenide. The reaction progress was monitored by ^{1}H NMR spectroscopy at 25 ºC. The relative

populations of DTT^{red} and DTT^{ox} were estimated by integration of the peaks at δ = 2.63 and 3.67

ppm of DTT^{red} and at δ = 2.87, 3.03, and 3.49 ppm of DTT^{ox}. The remaining amounts of DTT^{red}

are plotted in Figure 3 as a function of the reaction time. The times requisite for 50% conversion

of DTT^{red} to DTT^{ox} in CD_3OD (t_{50}) are summarized in the third column of Table 2.

In methanol, all selenides exhibited GPx-like antioxidant activity as in a phosphate buffer (i.e.,

in water), but the activity was remarkably enhanced in methanol compared to the blank. It is also

obvious that the activity varied largely depending on the structure and the substituents. When

cyclic selenides **4-7** are compared to open-chain selenide **1** (Figure 3A), it is seen that the

activities of five-membered ring selenides **4** and **6** are higher than that of **1**, while the activity of

four-membered ring selenide **5** is nearly equal to that of **1** and for the case of six-membered ring

selenide **7** it is even lower. The trend of the activities observed for the cyclic selenides are similar

to that observed in water, indicating that the ring-size effect on the GPx-like activity of cyclic

selenides is not affected by the solvent (i.e., the optimal ring-size is five). However, including

open-chain selenide **1**, the order of the activity in methanol (i.e., **7** < **1** ≈ **5** < **4** < **6**) is

significantly different from that observed in water (i.e., **1** < **7** < **5** < **4** ≈ **6**). Moreover, as to the

18

stereo configuration of the two OH substituents (i.e., **4** vs **6**) the effect is striking in methanol.

This is in large difference from the marginal effect observed in water. Thus, solvent effect would

be an important factor that can control the relative GPx-like activities of selenides.

In Figure 2B, the GPx-like activities of selenides **2**–**4** and **8**–**11** are compared to investigate

the effect of the substituents on the activity. When the selenides with two functional groups are

focused, the activity increases in the order of **3** ($CO_2H \times 2$) < **10** ($NH_2 \times 2$) < **4** ($OH \times 2$) < **2**

($NH_2 \times 2$) < **9** ($NH_2 \times 2$), showing that the substitution of the acidic functional groups (CO_2H)

with neutral (OH) or basic ones (NH_2) enhances the activity in methanol. In general, the

substituent effect on the GPx-like activity can be inverted in methanol from that in water[21]

because in water the substituent is protonated or deprotonated while it would exist as an

electronically neutral form in methanol. Comparison of the activity between **4** and **10**, however,

shows confliction to this general assumption. As to the effect of cyclization, it seems that the ring

structure basically increases the activity according to comparison of the activity between **2** (NH_2

$\times 2$) and **9** ($NH_2 \times 2$). However, **10** ($NH_2 \times 2$) and **8** ($NH_2 \times 1$) with five-membered ring structure

showed lower activity than open-chain selenide **2**. Moreover, cyclic diaminoselenolane with

trans configuration (**9**) exhibits the higher activity than the *cis*-isomer (**10**) in methanol. This

trend is opposite to the case of DHS (i.e., **4** vs. **6** in methanol). These results strongly suggest that

stereo configuration and a count of an NH_2 substituent have more complex effects on the

GPx-like activity in methanol than those in water. As to a CO_2H substituent, on the other hand,

19

the activity of **3** with linear structure is slightly higher than that of **11** with a six-membered ring.

This trend is consistent with that observed in water.

Based on the overall results obtained from the assays in water and in methanol, it is obvious

that the effects of substituents, including those of the count and the stereo configuration, on the

GPx-like antioxidant activity of selenides in methanol are significantly different from those in

water. This suggests the possibility that the activity can be controlled by changing the solvent.
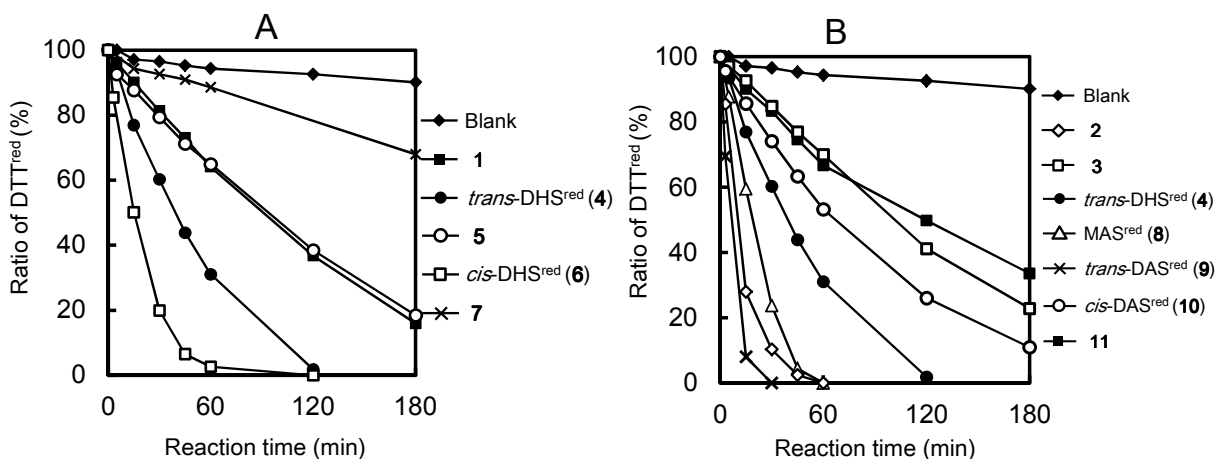
Figure 3: Percentages of residual DTT^{red} as a function of the reaction time in the oxidation of

DTT^{red} with H_2O_2 in the presence of a selenide catalyst (**1-11**) in CD_3OD. (A) A selenide catalyst

was **1**, **4**, **5**, **6**, or **7**. (B) A selenide catalyst was **2**, **3**, **4**, **8**, **9**, **10**, or **11**. Reaction conditions were

$[DTT^{red}]_0 = [H_2O_2]_0 = 0.14$ mM and [selenide] = 0.014 mM at 25 °C.

Competition of the reducing ability of selenides. Since the rate-determining step in the

GPx-like catalytic cycle of a selenide is the oxidation process with H_2O_2 to the selenoxide (i.e.

20

reaction A in Scheme 1),[21] the reducing ability of selenides should have strong correlation with

the GPx-like activity. To confirm this hypothesis, competitive oxidation of the selenides with

H_2O_2 in D_2O was monitored by ^{77}Se NMR. When selenides **4** and **5** were simultaneously

oxidized with one equivalent of H_2O_2 (Figure 4A), about 80% of **4** disappeared and the signal

corresponding to the selenoxide (*trans*-DHS^{ox}, **24**) appeared in a low magnetic field, while the

concentration of **5** decreased in only about 20%. The result indicated that the reducing ability of

a five-membered ring selenide is higher than that of a four-membered ring selenide. This is

consistent with the order of GPx-like activity observed for **4** and **5** in water (Figure 2).

Similarly, when oxidation of selenides **4** and **10** with H_2O_2 was compared in D_2O (Figure 4B),

4 was more readily oxidized than **10**. The result is again consistent with the order of the GPx-like

activity in water (Figure 2). A similar result was obtained in the competitive experiment using

selenides **4** and **9**. According to the results obtained from the competitive experiments for various

combinations of the selenides, the order of the reducing ability was eventually determined to be

3 ≈ **11** > **4** ≈ **6** ≈ **8** > **1** ≈ **5** ≈ **7** ≥ **9** ≈ **10** > **2**. This order is consonant with the order of the

GPx-like activity in an aqueous medium (Figure 2 and Table 2), strongly supporting the fact that

the rate-determining step in the GPx-like catalytic cycle of selenides is the oxidation process.

The same examination was taken place in CD_3OD as a solvent in order to obtain information

for the relationship between easiness of the oxidation step (reaction A in Scheme 1) and the

GPx-like activity in methanol (Figure 3). Surprisingly, the order of reducing ability of the

selenides in methanol was completely identical to that determined in water (i.e., **3** ≈ **11** > **4** ≈ **6** ≈

8 > **1** ≈ **5** ≈ **7** ≥ **9** ≈ **10** > **2**) and did not have any correlation with the order of the GPx-like

activity in methanol (i.e., **9** ≈ **10** > **2** > **8** > **4** > **6** > **5** ≈ **1** > **3** > **11** > **7**). This might be explained

by switching the rate-determining step of the catalytic cycle in methanol from reaction A to B.

However, it was confirmed that the reaction velocities for reaction A (~1 h) is obviously slower

than that for reaction B (<5 min) when the conversion between *trans*-DHS[red] (**4**) and

trans-DHS[ox] (**24**) was monitored by ^{1}H NMR. Although the oxidation velocity in methanol was

larger than that in water (~2 h), the rate-determining step was still reaction A in methanol.

Another possible reason for the observed discrepancy between the reducing ability of the

selenides and the GPx-like activity in methanol might be that the reaction progresses through a

different cycle from that shown in Scheme 1. Recently, Braga reported that the oxidation of

PhSH with H_2O_2 in methanol catalyzed by an aryl benzyl selenide/selenoxide redox system can

proceed via a hydroxy perhydroxy selenane intermediate, which is formed by further oxidation

of the selenoxide with H_2O_2.[24] Back reported formation of a spiro selenium species for similar

open-chain selenides.[23] Participation of such highly reactive species could explain the observed

discrepancy, but such species were not observed in our NMR analysis. At this moment, there is

no effective scenario to explain the order of the GPx-like activity observed for selenides **1-11** in

methanol.

22
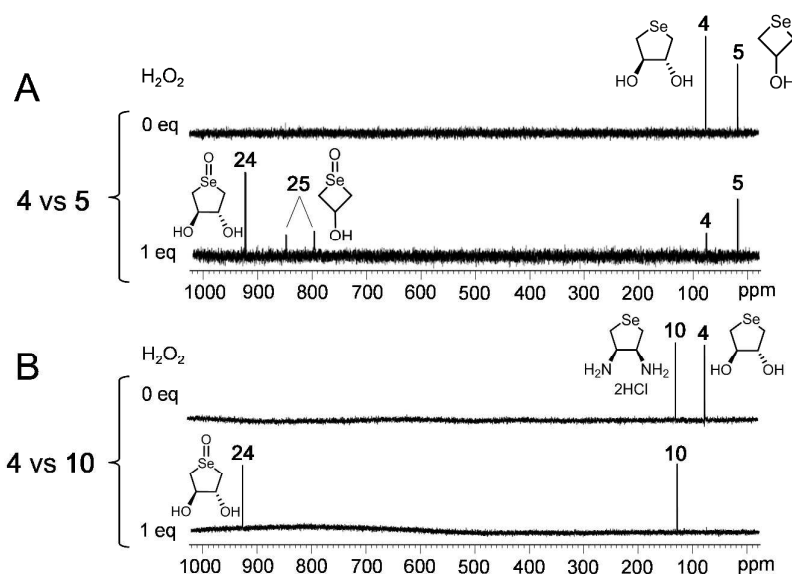
Figure 4: ^{77}Se NMR spectral changes observed for the competitive oxidation of (A) selenides **4**

and **5** (0.025 mmol each) and (B) selenides **4** and **10** (0.025 mmol each) with H_2O_2 (0.025 mmol)

in D_2O (0.7 mL) at 25 °C.

2.6. Second-order rate constants for reaction A

In order to further investigate the relationship between the reducing ability of selenides and

the GPx-like antioxidant activity in an aqueous medium, the second-order rate constants (k_{ox}) for

the oxidation of the selenides with H_2O_2 to the corresponded selenoxides (i.e. reaction A in

Scheme 1) were estimated as follows. It is known that the UV spectrum of a selenide changes

during the conversion to the selenoxide.[21] Indeed, the selenides employed in this study exhibited

clear UV spectral changes with a progress of the oxidation to the selenoxides. A representative

example is shown in Figure 5 for the case of oxidation of **9** to **20**. The reaction rate was then

determined by analyzing the time-course of the absorbance change at 234 nm. The second-order

rate constants (k_{ox}) for the oxidation of **1**, **2**, **3**, **4**, **8**, **9**, and **10** to the corresponding selenoxides

21, **22**, **23**, **24**, **28**, **20**, and **29**, respectively, were determined by plotting the observed pseudo

first-order rate constants (k_{obs}) against the concentration of H_2O_2 (Figure 6). The values of k_{ox}

estimated from the slopes are summarized in the fourth column of Table 2. The magnitude

decreases in the order, **3** > **4** > **8** > **1** > **9** ≈ **10** > **2**, which well matches with the order of the

GPx-like activity in an aqueous medium (i.e., **3** > **8** > **4** > **1** ≈ **9** ≈ **10** > **2**) except for the order of

4 and **8**. The correlation plots i.e., v_0 vs. k_{ox}, are shown in Figure 7. The positive correlation

confirmed that the reducing ability of a selenide can control the GPx-like activity in an aqueous

medium.

1
2
3
4
5
6
7
8
9
10
11
12
13
14
15
16
17
18
19
20
21
22
23
24
25
26
27
28
29
30
31
32
33
34
35
36
37
38
39
40
41
42
43
44
45
46
47
48
49
50
51
52
53
54
55
56
57
58
59
60
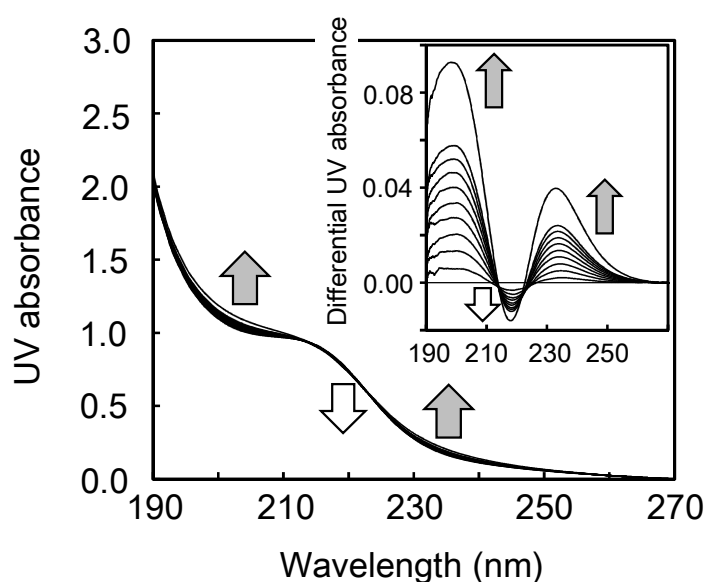
Figure 5: UV spectral changes (A) and differential UV spectra (B) observed in the oxidation of

selenide **9** with H_2O_2. Reaction conditions were $[9]_0 = 0.3$ mM and $[H_2O_2]_0 = 2$ mM in water at

25 °C. Reaction time was 0 to 50 min.
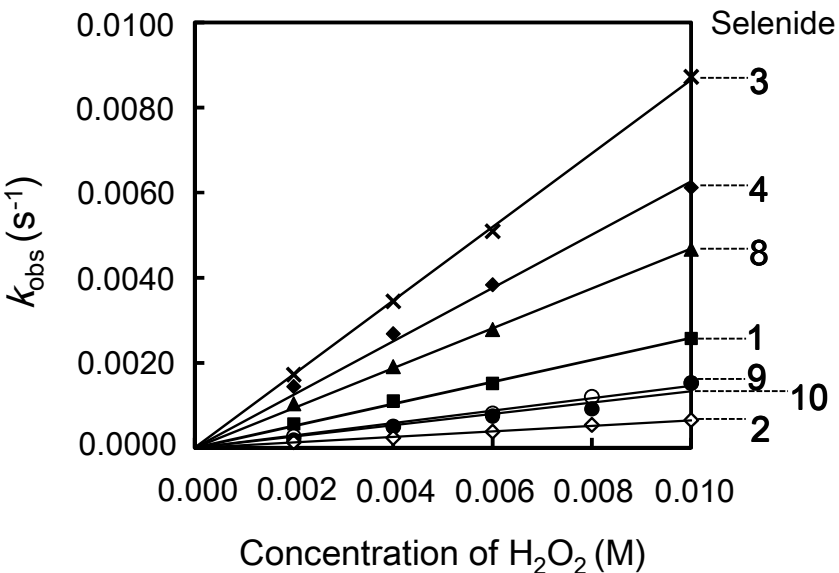
Figure 6: Linear plots showing the dependence of observed pseudo first-order rate constants

(k_{obs}) for the oxidation of selenide **1**, **2**, **3**, **4**, **8**, **9**, and **10** (0.3 mM) with H_2O_2.
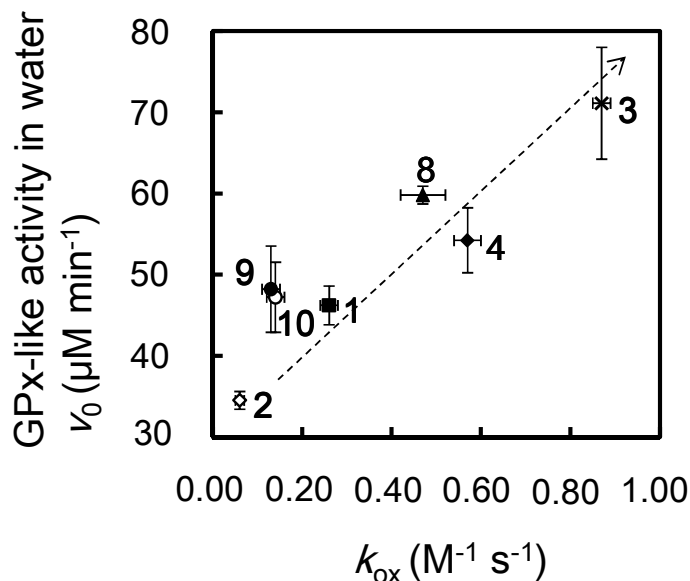
Figure 7: Correlation plot of the GPx-like activity (v_0) of selenides (**1**–**4** and **8**–**10**) in water vs. the second-order rate constants (k_{ox}) for the oxidation of selenides to the corresponding selenoxides.

HOMO energy levels The HOMO energy levels of selenides **1-11** were obtained by quantum chemical calculation at the B3LYP/6-31+G(d,p) level in vacuo and also in water applying the polarizable continuum model (PCM). The results are shown in the right side of Table 2. For all selenides, HOMO is dominantly localized at the selenium atom, indicating that the oxidation velocity of the selenides to the selenoxides should be controlled by the HOMO energy level.

Plots of the GPx-like activity observed for selenides **1-11** in methanol (i.e., the reaction times for 50% conversion of DTT[red], t_{50}) against the HOMO energy levels in vacuo failed to obtain a clear correlation curve (Figure 8). Thus, the GPx-like activity in methanol should not be

26

determined simply by the feasibility of the selenides to reduce H_2O_2. Despite this, there seems to

be a weak tendency that the higher HOMO results in the smaller t_{50} if one focuses on some series

of selenides. For example, the activity of open-chain selenides **1-3** increases with elevation of the

HOMO level (broken line a). Similar correlations seem to exist for DHS (**4** and **6**) and DAS (**9**

and **10**) series (broken lines b and c, respectively).
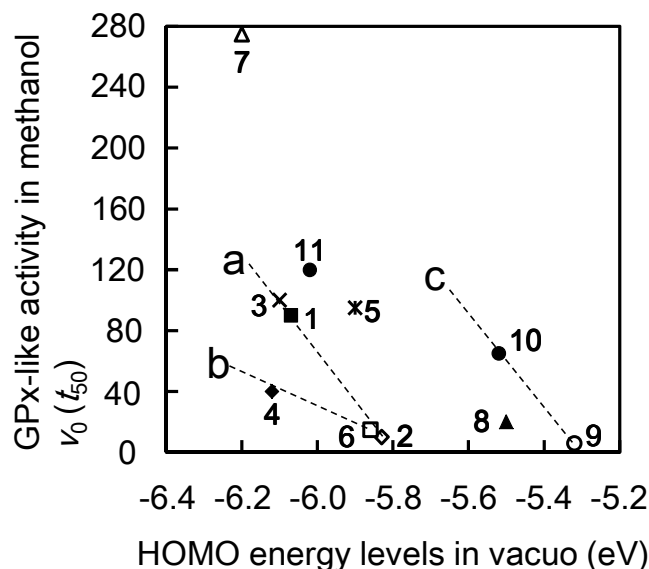
Figure 8: Correlation plots between HOMO energy levels of selenides **1-11** in vacuo and the

GPx-like activity in methanol (t_{50}).

On the other hand, a clear correlation was obtained in water between the HOMO energy level

and the GPx-like activity (v_0) as shown in Figure 9. The correlation supported that the GPx-like

antioxidant activity in water is controlled by the reducing ability of selenides. For the selenides

27

with NH$_2$ group(s), i.e., MAS^{red} (**8**), *trans*-DAS^{red} (**9**), and *cis*-DAS^{red} (**10**), however, the plots are obviously deviated from the correlation line. This may be explained by considering the equilibrium between an ionized form and a neutral form in water. If this equilibrium exists, the HOMO would be elevated and the plots should move toward the correlation line.
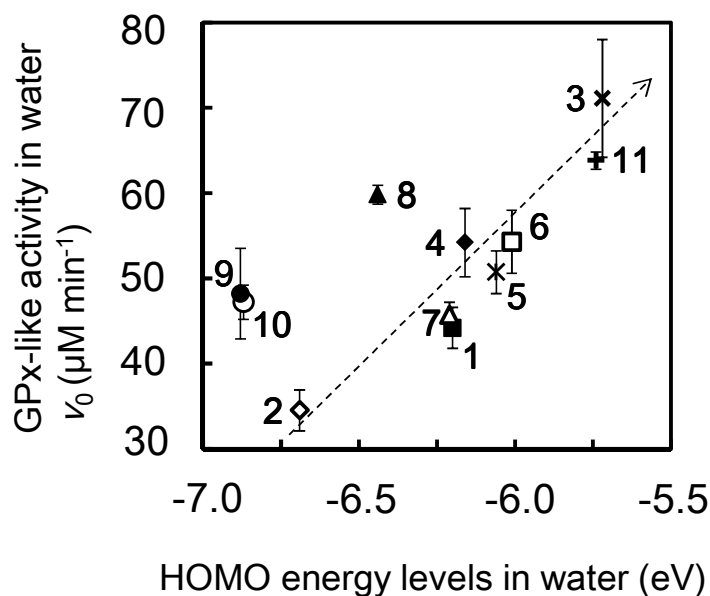
Figure 9: Correlation plots between HOMO energy levels of selenides **1-11** in water and the GPx-like activity in a phosphate buffer solution (v_0).

Conclusions

In this paper, we synthesized various series of water-soluble cyclic selenides **5-11** and compared their GPx-like antioxidant activities to reference selenides **1-4**. As a result, several

clues were obtained for molecular design of cyclic selenides with enhanced GPx-like activity. (1)

The optimal ring size would be five. (2) Substituents can control the activity. In general, the

activity increases by changing the substituent from NH_2 to OH and then CO_2H in water, but this

order is inverted in methanol. (3) The count of a substituent should also control the activity, but

this effect does not always hold because MAS^{red} (**8**) shows higher activity than DAS^{red} (**9** and **10**)

in water. (4) Stereo configuration of the substituents does not affect the activity in water, but it

would have a strong impact in methanol. (5) As to the solvent effects, the activity is enhanced in

methanol, but the rank of the activity in methanol cannot be explained by simple scenarios based

on the reducing ability of the selenides and the HOMO energy levels. Although more extensive

study is necessary to fully understand the observed GPx-like activity, especially in methanol,

these findings will be useful in future study for development of small molecular GPx mimics or

antioxidant selenium drugs.

Experimental Section

General. ^{1}H (500 MHz), ^{13}C (125.8 MHz), and ^{77}Se (95.4 MHz) NMR spectra were recorded

at 298 K and coupling constants (J) are reported in Hz. High-resolution mass spectra (HRMS)

were recorded under atmospheric pressure chemical ionization (APCI+) or electrospray

ionization (ESI+) conditions. All reactions for the synthesis of selenides were monitored by

thin-layer chromatography (TLC). Gel permeation chromatography (GPC) was performed with a

general isocratic HPLC system using CHCl₃ as an eluent. Ultra violet (UV) spectra were

measured at 25.0 °C by using a circulating water-bath system. Selenides **1**,[20] **2**,[20] **3**,[20] **4**,[27] **5**,[28]

7,[29,30] **8**,[31] and **11**[20] were prepared according as described. Compound **12**,[32] **17a**,[36] and **17b**[37–39]

were prepared by following previous literature procedures. All other chemicals were used as

purchased without further purification.

(*cis*-2,2-Dimethyl-1,3-dioxolane-4,5-diyl)dimethanol (14).[34] Diol **12** (990 mg, 3.3 mmol)

was mixed with 2,2-dimethoxypropane (DMP) (13.5 mL) and *p*-toluenesulfonic acid (*p*-TsOH)

(52 mg, 0.30 mmol). After stirring the mixture for 2 h at 35 °C, the solution was neutralize with a

saturated aqueous NaHCO₃ solution (40 mL) and further stirred for 1 h. The resulting solution

was extracted with EtOAc (30 mL×1). The organic layer was washed with brine (40 mL×1),

dried over MgSO₄, and concentrated under vacuum to give **13** as a slightly yellow oil. Yield:

1.12 g (96%); ^{1}H NMR (500 MHz, CDCl₃) δ 7.17 (m, 10H), 4.39 (q, *J*=18.3, 4H), 4.23 (m, 2H),

3.43 (m, 4H), 1.34 (s, 3H), 1.26 (s, 3H). The ^{1}H NMR spectroscopic data of **13** is in good

agreement with that reported in the literature.[33]

Then, **13** (2.97 g, 8.67 mmol) was subsequently dissolved in MeOH (18 mL) and vigorously

stirred for 24 h at room temperature in the presence of Pd/C as a catalysis under a hydrogen

atmosphere. The resulting solution was filtrated to remove Pd/C and concentrated in vacuo to

give **14** as colorless oil. Yield: 1.26 g (90%); ^{1}H NMR (500 MHz, CD$_3$OD) δ 4.25 (m, 2H), 3.67 (m, 4H), 1.44 (s, 3H), 1.36 (s, 3H); ^{13}C NMR (125.8 MHz, CD$_3$OD) δ 108.1, 77.4, 60.2, 26.8, 24.1.

(*cis*-2,2-Dimethyl-1,3-dioxolane-4,5-diyl)bis(methylene) dimethanesulfonate (15).[34] To a cooled (0 °C) solution of **14** (0.60 g, 3.68 mmol) in pyridine (3 mL) was slowly added methanesulfonyl chloride (MsCl) (855 μL, 11.0mmol). After stirring the mixture solution for 2.5 h at room temperature, 50 mM HCl (20 mL) was added and the solution was further stirred for 10 min. The resulting solution was extracted with EtOAc (25 mL×3) and then the organic layer was washed with water (20 mL×1) and brine (20 mL×1), dried over MgSO$_4$, and concentrated in vacuo. The obtained residual material was purified by silica gel column chromatography (EtOAc/*n*-Hexane 1:1) to give **15** as a white solid. Yield: 0.76 g (65%); R$_f$ 0.29 (EtOAc/*n*-Hexane 1:1); ^{1}H NMR (500 MHz, CDCl$_3$) δ 4.51 (m, 2H), 4.37 (m, 4H), 3.11 (s, 6H), 1.51 (s, 3H) 1.41(s, 3H); ^{13}C NMR (125.8 MHz, CDCl$_3$) δ 110.2, 74.2, 66.4, 37.7, 27.5, 25.1.

***cis*-3,4-Dihydroxy-tetrahydroselenophene (*cis*-DHS^{red}) (6)**.[35] Selenium powder (0.18 g, 2.28 mmol) and sodium borohydride (0.26 g, 6.87 mmol) were placed in a two-necked round-bottomed flask. After replacement of air with nitrogen gas in the flask, anhydrous EtOH (11 mL) was added. The mixture was stirred and heated under reflux conditions for 45 min to generate sodium hydrogen selenide (NaHSe) in situ. A solution of **15** (0.37 g, 1.16 mmol) in anhydrous THF (7 mL) was added to the resulting colorless solution through a glass syringe.

After heating under reflux conditions for 2.5 h, the mixture was cooled to room temperature and

extracted with EtOAc (25 mL ×3). The organic layer was washed with brine (40 mL ×1), and

dried over MgSO$_4$, and concentrated in vacuo. The residual yellow solid was purified by silica

gel column chromatography (EtOAc/ n-Hexane1:2) and then by GPC to give **16** as a white solid.

Yield: 160 mg (65%); mp 52.9–54.5 °C; R$_f$ 0.61 (EtOAc/ n-Hexane1:2); ^{1}H NMR (500 MHz,

CDCl$_3$) δ 4.84 (m, 2H), 2.94 (m, 4H), 1.46 (s, 3H) 1.26 (s, 3H); ^{13}C NMR (125.8 MHz, CDCl$_3$) δ

110.4, 84.5, 30.3, 26.4, 24.41; ^{77}Se NMR (95.4 MHz, CDCl$_3$) δ 162.8.

Then, an aqueous AcOH (4.5 mL, 80%) was added to a solution of **16** (0.16 g, 7.69mmol) in

MeOH (4.5mL). The mixture was vigorously stirred under reflux conditions for 16.5 h. The

resulting solution was evaporated to remove residual MeOH and azeotropically dried with

EtOAc (20 mL) to give **6** as a white solid. Yield: 0.13 g (quantitative); mp 78–80 °C; R$_f$ 0.51

(Et$_2$O/EtOAc1:1); ^{1}H NMR (500 MHz, D$_2$O) δ 4.22 (m, 2H), 2.93 (m, 2H), 2.65 (m, 2H); [13]C

NMR (125.8 MHz, D$_2$O) δ 76.1, 23.3; ^{77}Se NMR (95.4 MHz, D$_2$O) δ 83.6.

threo-**2,3-Bis(*tert*-butoxycarbonylamino)butane-1,4-diyl dimethanesulfonate (18a).** MsCl

(100 μL, 1.27 mmol) was slowly added to a cooled (0 °C) solution of **17a** (177 mg, 0.55 mmol)

in pyridine (5 mL). After stirring at 0 °C for 3.5 h. the resulting solution was poured into chilled

water (1 °C). Precipitates were filtrated under diminished pressure and dried overnight in the

atmosphere to give **18a** as a white solid material. Yield: 230 mg (88%); mp 103–107 °C, R$_f$ 0.65

(EtOAc/Hexane 1:2); ^{1}H NMR (500 MHz, CDCl$_3$): δ 5.19 (d, J=7.0, 2H), 4.26 (m, 4H), 4.02 (m,

2H), 3.00 (s, 6H), 1.38 (s, 18H); ^{13}C NMR (125.8 MHz, CDCl$_3$): δ155.9, 80.7, 68.1, 50.4, 37.5,

28.3; HRMS (APCI-TOF) m/z: [M + Na]$^+$ Calcd for C$_{16}$H$_{32}$N$_2$O$_{10}$S$_2$Na 499.1396; Found:

499.1423.

erythro-2,3-Bis(*tert*-butoxycarbonylamino)butane-1,4-diyl **dimethanesulfonate** **(18b).**

Compound **18b** was synthesized from **17b** (574 mg, 1.79 mmol) by a similar procedure to the

synthesis of **18a**. A white solid material. Yield: 775 mg (91%); mp 169–171 °C, R$_f$ 0.77

(EtOAc/Hexane 1:2); ^{1}H NMR (500 MHz, *d*-DMSO): δ 4.16 (m, 4H), 3.85 (s, 2H), 3.35 (s, 2H),

3.14 (s, 6H), 1.40 (s, 18H); ^{13}C NMR (125.8 MHz, *d*-DMSO): δ 155.7, 79.0, 69.4, 49.8, 37.1,

28.6; HRMS (APCI-TOF) m/z: [M + Na]$^+$ Calcd for C$_{16}$H$_{32}$N$_2$O$_{10}$S$_2$Na 499.1396; Found

499.1423.

trans-3,4-Bis(*tert*-butyloxycarbonylamino) **tetrahydroselenophene** **(19a).** Selenium

powder (103 mg, 1.12 mmol) and sodium borohydride (184 mg, 4.86 mmol) were placed in a

two-necked round-bottomed flask. After replacement of air with nitrogen gas in the flask,

anhydrous EtOH (8 mL) was added. The mixture was stirred and heated under reflux conditions

for 30 min under nitrogen atmosphere to generate sodium hydrogen selenide (NaHSe) in situ. A

solution of **18a** (190 mg, 0.40 mmol) in anhydrous THF (12 mL) was added to the resulting

colorless solution at 45 °C through a glass syringe. After heating under reflux conditions for 4 h,

water (40 mL) was added to the mixture and extraction was conducted with CH$_2$Cl$_2$ (50 mL × 3).

The combined organic layers were washed with brine (40 mL×1), dried over MgSO$_4$, and

33

concentrated under vacuum. The residual yellow solid was purified by silica gel column

chromatography (Et$_2$O/n-Hexane 2:1) and then by GPC to give **19a** as a white solid. Yield: 118

mg (81%); mp 193–194 °C; R$_f$ 0.33 (Et$_2$O/n-Hexane 2:1); ^{1}H NMR (500 MHz, CDCl$_3$): δ4.87 (s,

2H), 4.11 (s, 2H), 3.08 (m, 2H), 2.67 (m, 2H), 1.43 (s, 18H); ^{13}C NMR (125.8 MHz, CDCl$_3$): δ

155.6, 79.9, 59.0, 28.3, 23.4; ^{77}Se NMR (95.4 MHz, CDCl$_3$): δ 87.6; HRMS (APCI-TOF): m/z:

[M + Na]$^+$ Calcd for C$_{14}$H$_{26}$N$_2$O$_4$SeNa 389.0956; Found 389.0977.

cis-3,4-Bis(tert-butyloxycarbonylamino) tetrahydroselenophene (19b). Compound **19b**

was synthesized from **18b** (206 mg, 0.43 mmol) by a similar procedure to the synthesis of **19a**. A

white solid. Yield: 131 mg (83%); mp 136–138 °C; R$_f$ 0.29 (Et$_2$O/n-Hexane 2:1); ^{1}H NMR (500

MHz, CDCl$_3$): δ 5.16 (d, J=5.9, 2H), 4.27 (m, 2H), 3.17 (m, 2H), 2.56 (m, 2H), 1.42 (s, 18H);

^{13}C NMR (125.8 MHz, CDCl$_3$): δ 155.7, 79.9, 57.4, 28.3, 24.2; ^{77}Se NMR (95.4 MHz, CDCl$_3$): δ

104.5, 100.8; HRMS (APCI-TOF) m/z: [M + Na]$^+$ Calcd for C$_{14}$H$_{26}$N$_2$O$_4$SeNa 389.0956; Found:

389.0977.

trans-3,4-Diamine-tetrahydroselenophene·2HCl (trans-DAS^{red}) (9). 4 M HCl (2 mL) was

added to a solution of **19a** (33.0 mg, 0.09 mmol) in THF (2 mL). The mixture was vigorously

stirred for 18 h at room temperature. After removal of the ethereal layer by evaporation, the

aqueous solution was diluted with water (30 mL) and lyophilized to give **9** as a white powder.

Yield: 22.6 mg (quantitative); mp 199 °C (decomp); ^{1}H NMR (500 MHz, D$_2$O): δ 4.25 (m, 2H),

3.27 (m, 2H), 3.11 (m, 2H); ^{13}C NMR (125.8 MHz, D$_2$O): δ 57.6, 22.7; ^{77}Se NMR (95.4 MHz,

D_2O): δ 121.5; HRMS (APCI-TOF) m/z: [M + H − 2HCl]$^+$ Calcd for $C_4H_{11}N_2Se$ 167.0082;

Found 167.0043.

cis-3,4-Diamine-tetrahydroselenophene·2HCl (cis-DAS^{red}) (10). Compound **10** was

synthesized from **19b** (22.1 mg, 0.06 mmol) by a similar procedure to the synthesis of **9**. A white

powder. Yield: 14.1 mg (quantitative); mp 173 °C (decomp); ^1H NMR (500 MHz, D_2O): δ 4.21

(m, 2H), 3.30 (m, 2H), 2.90 (m, 2H); ^{13}C NMR (125.8 MHz, D_2O): δ 57.6, 30.3; ^{77}Se NMR (95.4

MHz, D_2O): δ 121.5; HRMS (APCI-TOF) m/z: [M + H − 2HCl]$^+$ Calcd for $C_4H_{11}N_2Se$

167.0082; Found 167.0043.

NADPH-coupled GPx activity assay using GSH as a thiol substrate.[40] A test solution was

prepared by mixing a 100 mM phosphate/6 mM EDTA buffer solution (1941 μL) at pH 7.4

containing NADPH (2.0 μmol) and GSH (6.8 μmol) with a GR solution (453 U/mL, 59 μL). An

aliquot (300 μL) of the test solution was added to a 1.0 mM selenide solution (200 μL) in 100

mM phosphate buffer at pH 7.4, and the resulting solution was diluted with the phosphate buffer

solution (430 μL) and maintained at 25 °C. The reaction was initiated by addition of a 36 mM

aqueous H_2O_2 solution (70 μL) to the mixture solution. The reaction progress was monitored by

absorption change at 340 nm due to consumption of NADPH. The initial concentrations of the

selenide, H_2O_2, GSH, NADPH, and GR in the assay solution were 0.2 mM, 2.5 mM, 1.0 mM,

0.3 mM, and 4 U/mL, respectively.

GPx activity assay using DTT^{red} as a dithiol substrate. The activity assay was performed

35

by following the literature.[20] DTT^{red} (0.15 mmol) and selenide (0.015 mmol) were dissolved in

CD$_3$OD (1.1 mL), and the solution was added with 30% H$_2$O$_2$ (17 μL, 0.15 mmol) to start the

reaction. ^{1}H NMR spectra were measured at a variable reaction time at 25 °C. The relative

populations of DTT^{red} and DTT^{ox} were determined by integration of the ^{1}H NMR absorptions

that were well isolated on the spectrum.

Kinetic Analysis. The velocity (k_{obs}) of the reaction between H$_2$O$_2$ (2.0 ∼ 10.0 mM) and

selenide (0.3 mM) was measured at 25 °C in water by following the UV absorption change at

225, 228, 221, 225, 222, 234, or 236 nm for selenides **1**, **2**, **3**, **4**, **8**, **9**, and **10**, respectively. The

measurement was repeated more than three times. The obtained k_{obs} values were then plotted

against the concentration of H$_2$O$_2$ to determine the second order rate constants (k_{ox}) for reaction

A in Scheme 1.

Quantum chemical calculation. A Gaussian 09 software package (revision B.01)[41] was

employed. The structures were optimized in vacuo and in water at the B3LYP/6-31+G(d,p) level.

The polarizable continuum model (PCM)[42–45] was applied for the calculation in water. For the

linear selenides (**1-3**), an extended conformation with all dihedral angles *anti* was employed as

an initial structure. For the cyclic selenides (**4-11**), all possible stereo configurations were tested,

and the obtained global energy structure was applied for the analysis of experimental data.

Frequency calculation was performed for the obtained energy minimum structures to confirm

that the structure has no imaginary frequency. The structures thus obtained were used for

36

analyzing the energy levels and the shapes of the molecular orbitals.

Acknowledgments

Supporting information

^{1}H and ^{13}C NMR spectra of compounds, **6**, **9**, **10**, **13–16**, **18a**, **18b**, **19a**, and **19b**, ^{1}H NMR spectra change in the redox reactions of selenide **9** and selenoxide **20**, structures optimized by quantum chemical calculations. This material is available free of charge via the Internet at http://pubs.acs.org.

References

(1)   Böck, A.; Forchhammer, K.; Heider, J.; Leinfelder, W.; Sawers, G.; Veprek, B.; Zinoni, F.

Mol. Microbiol. **1991**, *5*, 515–520.

37

(2)   Flohé, L.; Günzler, W. A.; Schock, H. H. *FEBS Lett.* **1973**, *32*, 132–134.

(3)   Savaskan, N. E.; Ufer, C.; Kühn, H.; Borchert, A. *Biol. Chem.* **2007**, *5*, 1007–1017.

(4)   Conrad, M.; Schneider, M.; Seiler, A.; Bornkamm, G. W. *Biol. Chem.* **2007**, *388*, 1019–

1025.

(5)   Toppo, S.; Flohé, L.; Ursini, F.; Vanin, S.; Maiorino, M. *Biochim. Biophys. Acta. Gen.*

Subj. **2009**, *1790*, 1486–1500.

(6)   Bhabak, K. P.; Mugesh, G. *Acc. Chem. Res.* **2010**, *43*, 1408–1419.

(7)   Alberto, E. E.; do Nascimento, V.; Braga, A. L. *J. Braz. Chem. Soc.* **2010**, *21*, 2032–2041.

(8)   Huang, X.; Liu, X.; Luo, Q.; Liu, J.; Shen, J. *Chem. Soc. Rev.* **2011**, *40*, 1171–1184.

(9)   Santi, C.; Tidei, C.; Scalera, C.; Piroddi, M.; Galli, F. *Curr. Chem. Biol.* **2013**, *7*, 25–36.

(10)   Mugesh, G. *Curr. Chem. Biol.* **2013**, *7*, 47–56.

(11)   Iwaoka, M. *Antioxidant organoselenium molecules.* In *Organoselenium chemistry between*

synthesis and biochemistry; Santi, C., Ed.; Publisher: Bentham Science Publishers, Sharjah,

2014, Chapter 12, pp. 361–378.

(12)   Wilson, S. R.; Zucker, P. A.; Huang, R. R. C.; Spector, A. *J. Am. Chem. Soc.* **1989**, *111*,

5936–5939.

(13)   Iwaoka, M.; Tomoda, S. *J. Am. Chem. Soc.* **1994**, *116*, 2557–2561.

(14)   Bhabak, K. P.; Mugesh, G. *Chem. Eur. J.* **2008**, *14*, 8640–8651.

(15)   Mugesh, G.; Panda, A.; Singh, H. B.; Butcher, R. J. *Chem. Eur. J.* **1999**, *5*, 1411–1421.

38

(16)   Wirth, T. *Molecules* **1998**, *3*, 164–166.

(17)   Collins, C. A.; Fry, F. H.; Holme, A. L.; Yiakouvaki, A.; Al-Qenaei, A.; Pourzand, C.;

         Jacob, C. *Org. Biomol. Chem.* **2005**, *3*, 1541–1546.

(18)   Prabhu, C. P.; Phadnis, P. P.; Wadawale, A. P.; Priyadarsini, K. I.; Jain, V. K. *J. Organomet.*

         Chem. **2012**, *713*, 42–50.

(19)   Nascimento, V.; Ferreira, N. L.; Canto, R. F. S.; Schott, K. L.; Waczuk, E. P.; Sancineto, L.;

         Santi, C.; Rocha, J. B. T.; Braga, A. L. *Eur. J. Med. Chem.* **2014**, *87*, 131–139.

(20)   Iwaoka, M., Kumakura, F. *Phosphorus Sulfur Silicon Relat. Elem.* **2008**, *183*, 1009–1017.

(21)   Kumakura, F.; Mishra, B.; Priyadarsini, K. I.; Iwaoka, M. *Eur. J. Org. Chem.* **2010**, 440–

         445.

(22)   Rahmanto, A. S.; Davies, M. J. *Free Radic. Biol. Med.* **2011**, *51*, 2288–2299.

(23)   Back T. G.; Moussa Z.; Parvez, M. *Angew. Chem. Int. Ed.* **2004**, *43*, 1268–1270.

(24)   Nascimento, V.; Alberto, E. E.; Tondo, D. W.; Dambrowski, D.; Detty, M. R.; Nome, F.;

         Braga, A. L. *J. Am. Chem. Soc.* **2012**, *134*, 138–141.

(25)   Prabhu, P.; Bag, P. P.; Singh, B. G.; Hodage, A.; Jain, V. K.; Iwaoka, M.; Priyadarsini, K. I.

         Free Radic. Res. **2011**, *45*, 461–468.

(26)   Arai, K.; Dedachi, K; Iwaoka, M. *Chem. Eur. J.* **2011**, *17*, 481–485.

(27)   Iwaoka, M.; Takahashi, T.; Tomoda, S. *Heteroatom Chem.* **2001**, *12*, 293–299.

(28)   Polson, G.; Dittmer, D. C. *J. Org. Chem.* **1988**, *53*, 791–794.

(29) Crombez-Robert, C.; Benazza, M.; Fréchou, C.; Demailly G. *Carbohydr. Res.* **1997**, *303*, 359–365.

(30) Szczepina, M. G.; Johnston, B. D.; Yuan, Y.; Svensson, B.; Pinto, B. M. *J. Am. Chem. Soc.* **2004**, *126*, 12458–12469.

(31) Arai, K.; Moriai, K.; Ogawa, A.; Iwaoka, M. *Chem. Asian J.* **2014**, *9*, 3464–3471.

(32) Nishizono, N.; Akama, Y.; Agata, M.; Sugo, M.; Yamaguchi, Y.; Oda, K. *Tetrahedron* **2011**, *67*, 358–363.

(33) Balamurugan, R.; Kothapalli, R. B.; Thota, G. K. *Eur. J. Org. Chem*. **2011**, 1557–1569.

(34) Nishizono, N.; Babe, R.; Nakamura, C.; Oda, K.; Machida, M. *Org. Biomol. Chem.* **2003**, *1*, 3692–3697.

(35) Nakayama, J.; Shibuya, M.; Ikuina, Y.; Murai, F.; Hoshino, M. *Phosphorus Sulfur Silicon Relat. Elem.* **1988**, *38*, 149–155.

(36) Martin, R. L.; Norcross, B. E. *J. Org. Chem.* **1975**, *40*, 523–524.

(37) Wu, F.-L.; Ross, B. P.; McGeary, R. P. *Eur. J. Org. Chem.* **2010**, 1989–1998.

(38) Scheurer, A.; Mosset, P.; Saalfrank, R. W. *Tetrahedron:Asymmetry* **1997**, *8*, 1243–1251.

(39) Lee, S. H.; Kohn, H. *J. Am. Chem. Sco.* **2004**, *126*, 4281–4292.

(40) Pascual, P.; Martinez-Lara, E.; Bárcena, J. A.; López-Barea, J.; Toribio, F. *J. Chromatogr. B: Biomed. Sci. Appl.* **1992**, *581*, 49−56.

(41) Gaussian 09, Revision B.01, M. J. Frisch, G. W. Trucks, H. B. Schlegel, G. E. Scuseria, M.

40

A. Robb, J. R. Cheeseman, G. Scalmani, V. Barone, B. Mennucci, G. A. Petersson, H. Nakatsuji, M. Caricato, X. Li, H. P. Hratchian, A. F. Izmaylov, J. Bloino, G. Zheng, J. L. Sonnenberg, M. Hada, M. Ehara, K. Toyota, R. Fukuda, J. Hasegawa, M. Ishida, T. Nakajima, Y. Honda, O. Kitao, H. Nakai, T. Vreven, J. A. Montgomery, Jr., J. E. Peralta, F. Ogliaro, M. Bearpark, J. J. Heyd, E. Brothers, K. N. Kudin, V. N. Staroverov, T. Keith, R. Kobayashi, J. Normand, K. Raghavachari, A. Rendell, J. C. Burant, S. S. Iyengar, J. Tomasi, M. Cossi, N. Rega, J. M. Millam, M. Klene, J. E. Knox, J. B. Cross, V. Bakken, C. Adamo, J. Jaramillo, R. Gomperts, R. E. Stratmann, O. Yazyev, A. J. Austin, R. Cammi, C. Pomelli, J. W. Ochterski, R. L. Martin, K. Morokuma, V. G. Zakrzewski, G. A. Voth, P. Salvador, J. J. Dannenberg, S. Dapprich, A. D. Daniels, O. Farkas, J. B. Foresman, J. V. Ortiz, J. Cioslowski, and D. J. Fox, Gaussian, Inc., Wallingford CT, **2010**.

(42) Cancès, E.; Mennucci, B.; Tomasi, J. *J. Chem. Phys.* **1997**, *107*, 3032–3041.

(43) Mennucci, B.; Tomasi, J. *J. Chem. Phys.* **1997**, *106*, 5151–5158.

(44) Mennucci, B.; Cancès, E.; Tomasi, J. *J. Phys. Chem. B* **1997**, *101*, 10506–10517.

(45) Tomasi, J.; Mennucci, B.; Cancès, E. *J. Mol. Struct. THEOCHEM* **1999**, *464*, 211– 226.